

Research Article

# Construction and Application of “Active Prediction-Passive Warning” Joint Impact Ground Pressure Resilience Prevention System: Take the Kuan Gou Coal Mine as an Example

Jiantao Cao <sup>1,2</sup>, Shuai Zhang <sup>1</sup>, Huicong Xu <sup>1</sup>, Wei Li<sup>1</sup> and Jindong Wang <sup>3</sup>

<sup>1</sup>College of Energy Science and Engineering, Xi'an University of Science and Technology, Xi'an, Shaanxi 710054, China

<sup>2</sup>Key Laboratory of Western Mines and Hazard Prevention of China Ministry of Education, Xi'an University of Science and Technology, Xi'an, Shaanxi 710054, China

<sup>3</sup>School of Energy Engineering, Yulin University, China

Correspondence should be addressed to Shuai Zhang; [zscsy1993@163.com](mailto:zscsy1993@163.com)

Received 2 July 2022; Revised 20 October 2022; Accepted 25 October 2022; Published 20 February 2023

Academic Editor: Shaofeng Wang

Copyright © 2023 Jiantao Cao et al. Exclusive Licensee GeoScienceWorld. Distributed under a Creative Commons Attribution License (CC BY 4.0).

With the increasing depth and intensity of coal mining, the impact on ground pressure has become one of the main disasters facing mining, seriously threatening mine safety. Introducing the concept of toughness urban design, building a joint toughness prevention and control system based on active prediction and analysis of the impact pressure risk at the back mining face according to the geological deposit conditions and mining technology conditions and passive warning using monitoring data to explore the impact precursor characteristics is an important basis for impact pressure management and has important engineering significance to ensure the safe back mining. In this paper, firstly, the whole working face is divided into small unit areas, and the BP neural network prediction model is constructed to predict and analyze each small unit separately, and the distribution of impact ground pressure hazard level in different areas of the working face is derived. Next, a FLAC numerical model was established to analyze the stress distribution and migration characteristics at different retrieval distances of the working face and to explore the main distribution areas of impact hazard. Finally, the trend method, critical value method, and dynamic rate of change method were applied to determine the early warning indicators of impact ground pressure in the Kuan Gou coal mine, establish a comprehensive early warning method of impact ground pressure applicable to the Kuan Gou coal mine, and carry out field application with good effect. The findings of this paper have good scientific significance and reference value for promoting impact hazard analysis and early warning in mines with similar geological conditions and mining technology conditions in China.

## 1. Introduction

The rapid development of society is inseparable from the drive for energy, the double carbon policy has intensified the demand for efficient and clean use of energy, and coal as the cornerstone of China's current energy is still in the dominant position of energy [1, 2]. After the coal resources enter into deep mining, the special environment of “three highs and one disturbance” inevitably produces the phenomenon of dynamic disasters, which seriously threatens the mining and related engineering construction in China, among which the impact of ground pressure represents a frequent and

significant impact [3–5]. Researchers at home and abroad have also conducted extensive research on it and put forward various academic views, gradually refining the disaster-causing mechanism of impact ground pressure. At present, a more complete anti-impact technology system has been explored based on a large number of engineering practices, but the complexity of the formation mechanism of impact ground pressure and other factors still needs to be explored in depth; especially, deep coal mining has a significant urgency and necessity and has great scientific and practical significance to achieve the safe and efficient development of deep resources and underground space maintenance [6–10].

The concentration of stress causes energy focus and the presence of a weak surface is a prerequisite for the formation of impact ground pressure. The study findings suggest that the accumulation and release of energy in the coal rock body is reasonable or not, which directly determines whether the impact ground pressure can be accurately warned and effectively controlled [11, 12]. To better interpret the impact of ground pressure prevention and control early warning mechanism, this paper addresses the actual situation of the Kuan Gou coal mine; firstly, according to the geological endowment of the working face and mining technology conditions, analyze the impact of these factors on the impact ground pressure, analyze the impact hazard of the working face, and divide the high-frequency area of the impact hazard of the working face [13–15]. Secondly, microseismic monitoring data were used to explore the precursor response characteristics of the data; finally, sensitive indicators for impact ground pressure early warning in the Kuan Gou coal mine were selected to establish a comprehensive impact ground pressure early warning method applicable to the actual situation in Kuan Gou coal mine, and the field application was effective. The research results have important theoretical value and engineering significance for improving the early warning mechanism of impact ground pressure.

## 2. Engineering Background

The prevention and control of impact pressure in the Kuan Gou coal mine are not only influenced by the geological conditions of the mine but also by the technical conditions of production. The analysis of geological conditions and production technology conditions of the Kuan Gou coal mine understands the real situation of the mine, selects the main geological influencing factors of impact pressure, divides the impact hazard area of the working face, provides a reference for the effective prevention and control of impact pressure in the early stage, and provides a reliable basis for the subsequent study of early warning and comprehensive key prevention and control of impact pressure in the Kuan Gou coal mine.

*2.1. Introduction to the Mine.* The Kuan Gou coal mine is a subsidiary of Xinjiang Energy Company Limited, which is located in the town of Quergou, Hutubi County, Changji Prefecture. The topography of the mine is high in the south and low in the north and high in the west and low in the east, with exposed bedrock in the south, and the topographic slope changes from steep in the south to gentle in the north, influenced by the near east-west direction of the Baiyanggou River, which cuts through the eastern part of the Kuan Gou mine area in the north direction of the Hutubi River, the lowest terrain area. Green grass vegetation is well-developed in most of the northern part of the coal mine. The highest point in the south, Baiyanggou Dasaka, is 1914.2 m above sea level, and the lowest point is Hutubi River at an elevation of 1185 m, with the range of relative height difference generally between 200 and 350 m.

*2.2. Working Face Overview.* W1123 comprehensive mining topping coal working face is located in the B<sub>2</sub> coal seam in the west wing of the first mining area, the inclined length of the working face is 192 m, the recoverable length is 1468 m, the mining height is 3.2 m, the thickness of coal released is 6.3 m, the recoverable area is 282048 m<sup>2</sup>, and the inclination angle of the working face is 14° on average. The first mining face of the B<sub>2</sub> coal seam is located in the west wing of the first mining area, the west wing mining area is divided into two sections of working face because the upper section working face is near the mine boundary, and there are small kiln mining area and geological structure, which need to be further explored. W1123 working face is located in the B<sub>2</sub> coal seam on the west side of the track hill, and 15 m downward of the same seam is the W1121 mining area; the upper 50 m near 700 m to the east of the open-cut road is the W1145 mining area of B<sub>4-1</sub> coal seam open-cutting road; 54 m south of the working face is B<sub>2</sub> mining area which is suspected to be the border small kiln trans-boundary mining coal seam.

*2.3. Analysis of Disaster-Causing Factors of Impact on Ground Pressure.* After a large number of previous studies, the mechanism of impact ground pressure has become clear. In terms of mechanical essence, impact ground pressure is a nonlinear kinetic process of energy accumulation in the steady state and release in the unsteady state in the process of deformation and destruction of the coal-rock system under specific geological conditions, which is a comprehensive reflection of its external loading environment, internal structure, tectonics, and its physical and mechanical properties, and has obvious spatial and temporal evolutionary characteristics [16].

Impact pressure is a complex problem influenced by various factors; the main factors can be summarized into two categories: geological and mining technology factors. Geological factors are the basic conditions affecting impact pressure that are objective and difficult to change, while mining technology factors are influenced by mine size, the recovery process, interlayer layout, and other factors, which can be regulated through technical optimization.

According to the review of the literature related to the impact of ground pressure in the Kuan Gou coal mine, we understand the location of the major impact events and the extent of impact damage, as shown in Table 1.

Based on the impact events in Kuan Gou, the scene case of rock burst accident is shown in Figure 1, it is known that several impact ground pressure events occurred in the back mining of the B<sub>4</sub> coal seam, and the impact ground pressure disaster has become the main disaster in the mine, which brings new challenges to the normal back mining of the working face, personnel safety, and equipment maintenance. Moreover, W1123 is in the B<sub>2</sub> coal seam, the working face is deeper than W1145, and the integrated mining process is more complicated than the integrated mining process used in the B<sub>4</sub> coal seam. To ensure the normal recovery of the W1123 working face, the prevention and control of impact pressure are more targeted, and the comprehensive early warning in the early stage is very important and can be used

TABLE 1: Description of historical shock events.

No.	Time of occurrence	Place of occurrence	Description of the impact situation
1	October 8, 2010	W1143	The first impact ground pressure accident in the history of Xinjiang occurred in the lower part of the W1143 working face (mining depth 317 m), with a protruding coal volume of 247 m <sup>3</sup> at the working face, resulting in serious consequences of multiple deaths and scrapping of coal mining machines and several hydraulic supports.
2	July 4, 2011	E1146	An impact pressure accident occurred about 5 m behind the E1146 backwind tunnel boring face, the tunnel section contracted sharply, the header was squeezed into the tunnel gang, and the driver was shaken up and fell behind the header.
3	July 6, 2011	E1146	A similar impact ground pressure accident occurred again in the E1146 backwind tunnel boring face.
4	January 9, 2013	E1148	Impact pressure occurred in the E1148 backwind tunneling face (buried depth of 300 m) when it was dug to 910 m. Accompanied by a strong coal explosion sound, the coal wall deformed sharply, the coal gang bulged out as a whole, the anchor rod failed, the bottom drum amounted to 800 mm, and the impact area was about 10 m.
5	January 12, 2013	E1148	A similar impact pressure accident occurred again in the E1148 backwind tunnel boring face.



(a) Coal mining machine rocker arm breakage



(b) Hydraulic support column breakage

FIGURE 1: Damage from the “October 8, 2010,” impact ground pressure disaster.

as the basis for the prevention and control of impact pressure in the later stage.

### 3. Active Prediction Technique Based on the Combination of Neural Network and Numerical Simulation

*3.1. BP Neural Network Picks Up Impact Hazard Areas.* BP neural networks are widely used in several fields for their strong nonlinear mapping ability, and neural networks have been able to handle nonlinear types of problems very well [17].

According to the actual engineering and site experience, the classification of the risk level of impact ground pressure and the approximate measures that should be taken in the back mining mines at different risk levels are shown in Table 2.

*3.1.1. The BP Neural Network Model Construction.* The main feature of BP neural network prediction is the transmission of error in the opposite direction during the forward transmission of the signal, the backward propagation of the error according to the set network of the prediction error, and the automatic correction of the operation of the data through the feedback network of the error, the reanalysis of the oper-

ation process of the data simulation, the resulting results, and the set error range for comparison and analysis of the artificial intelligence algorithm [18–20]. The key work of the BP neural network structure is the setting of two aspects: the number of network layers and the number of nodes in each layer. In this paper, a 3-layer BP network model with one hidden layer is used. The parameters of the input and output of the network model are as follows: the input layer parameters have 7 parameters such as mining depth, coal seam thickness, coal seam inclination, roof management, tectonic situation, coal seam thickness change, and coal seam inclination change; the output layer has 4 nodes, which represent 4 impact levels of impact ground pressure at the working face; whether the number of nodes in the hidden layer is chosen reasonably has an important influence on the accuracy of the prediction results of the built network. The evaluation basis of impact factors of rock burst is shown in Table 3. The number of nodes in the hidden layer has an important influence on the accuracy of the prediction results of the constructed network, and the accuracy of the operation results cannot be guaranteed when the number of nodes is chosen to be small. Therefore, the number of nodes in the hidden layer of this network is determined to be 15.

TABLE 2: Classification of impact ground pressure hazard class.

Classification	Impact level	Impact on production activities
I	Micro-shock	All mining work can be carried out according to the operating procedures.
II	Weak impact	All mining work can be carried out according to the operating procedures. Observation of impact ground pressure hazard status is enhanced during operations.
III	Moderate impact	The next step of mining should be carried out together with the impact pressure prevention and control measures for this risk condition, and the impact pressure risk level should not be increased by the forecast.
IV	Strong impact	Mining operations should be stopped and unnecessary personnel should be evacuated from the dangerous location; the mining leader should determine the methods and measures to control the risk of impact pressure, as well as the inspection methods of the control measures, and determine the person who will participate in the prevention and control measures; after taking the measures and passing the expert appraisal, the next step of the operation can be carried out. If the risk of impact pressure is not reduced, the mining operation will be stopped and the area will be closed to traffic.

TABLE 3: Selection of values of impact ground pressure influencing factors.

Assignment	Constructed situation	Roof management	Coal thickness variation	Inclination change
0	Simple	Good	No change	No change
1	General	Better	Small	Small
2	More complex	Fair	Comparatively large	Comparatively large
3	Complicated	Poor	Large	Large

TABLE 4: Training functions and parameters.

Data selection	Deliver functions	Transfer functions	Training functions	Number of training sessions/session	Target accuracy	Learning rate
Selected values	Tensing	Purlin	Trained	5000	$1 \times 10^{-3}$	0.01

3.1.2. *Prediction Sample Acquisition and Processing.* The establishment of the BP neural network prediction model requires sufficient data samples, and according to the relevant literature, 24 sets of data from actual situations are selected as the training samples and test samples of the prediction model. The specific data are not listed. According to the original data, the mining depth, coal thickness, and inclination angle can be obtained values by the actual situation. The maximum value of mining depth is 633 m and the minimum is 278 m; the maximum value of dip angle is  $35^\circ$  and the minimum is  $3^\circ$ ; the maximum value of coal thickness is 12.0 m and the minimum is 3.0 m; the four impact ground pressure influencing factors of the tectonic situation, roof management, coal thickness change, and dip angle change are state quantities, which need to be quantified, and the specific values are selected as shown in Table 4. The impact ground pressure hazard class is divided into four impact cases of microimpact, weak impact, medium impact, and strong impact denoted by (1 0 0 0), (0 1 0 0), (0 0 1 0), and (0 0 0 1), respectively. The data are normalized for the sake of the fast operation of the model.

3.1.3. *Model Training and Validation.* Many typical neural network frameworks and functions have been constructed in the Matlab software toolbox, and the complex process of

building neural networks has been simplified by selecting the relevant training procedures in the software. The problem faced by the network model creator is mainly the understanding of the main features of the functional modules; then, according to the scope of application, advantages, and disadvantages of different functional modules and the characteristics of the research problem, the calculation function applicable to the object of study is selected and the parameters of the corresponding function are set, which improves the efficiency in the process of using Matlab software. The functions, algorithms, and training parameters selected for network training are shown in Table 4, and the training process is shown in Figure 2.

After the network training was completed, the data samples were used to verify whether the network prediction results meet the accuracy requirements, and the test results are shown in Table 5. According to the accuracy of the test error, it is known that the neural network has good accuracy in predicting the impact of ground pressure, and the actual situation can reach the accuracy of the actual activities of production when compared with the arithmetic results.

3.2. *Numerical Simulation to Identify the Impact Hazard of Working Face Recovery.* Mine production activities cause damage to the equilibrium of the coal rock body, and the



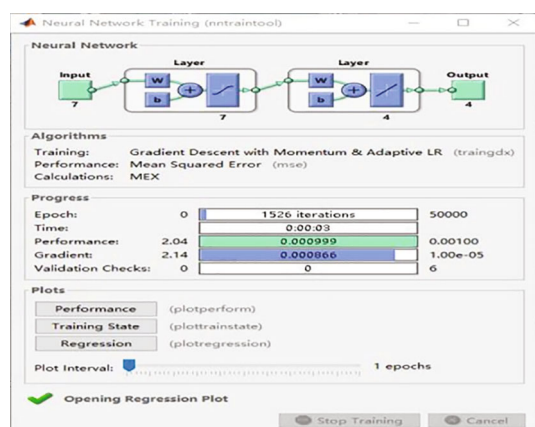


FIGURE 2: Neural network training process.

TABLE 5: Comparison of test results and actual values.

No.	Actual value	Test results	Mean square error
21	1 0 0 0	1.0000 0.0038 0.1276 0.0000	0.001
22	0 1 0 0	0.0000 0.9692 0.0026 0.0000	
23	0 0 0 1	0.0012 0.0000 0.0232 0.9338	
24	0 0 1 0	0.0005 0.0023 0.9795 0.0000	

redistribution of stress tends to form a high-stress concentration area. When the elastic energy accumulated in the coal rock body in the high-stress area exceeds the bearing limit, the sudden release of a large amount of elastic energy will induce the occurrence of impact ground pressure. According to the “force source factor” in the “three-factor” theory, the force source factors that induce impact ground pressure can be attributed to high-stress concentration and disturbance, and the mining layout is not reasonable to form a stress concentration area.

According to the actual situation of the working face, the coal pillars left in the process of upper coal recovery and the lateral support pressure on the adjacent part of this working face after the mining of the same coal will form a stress concentration effect on the W1123 recovery working face, and there are force source factors that induce impact ground pressure. With the continuous improvement of computer technology level, FLAC is widely used in the simulation analysis of structural stress characteristics. According to the physical and mechanical parameters of the coal rock body and the geological endowment conditions in which the working face is located, combined with the actual working face retrieval sequence, interlayer relationship, and other actual conditions in the Kuan Gou coal mine, numerical models of the working face coal rock are established to analyze the stress accumulation and migration characteristics, explore the high-stress distribution under the influence of mining disturbance in the retrieval working face, delineate the dynamic pressure hazard range, and provide a reference basis for more targeted prevention and control of impact ground pressure to reduce or avoid the occurrence of safety

accidents with impact ground pressure as the source of disaster.

**3.2.1. Working Face Recovery Model Construction.** The finite difference method was selected for the model calculation, and the corresponding numerical calculation model was established as shown in Figure 3 based on the geological column diagram of the Kuan Gou coal mine and the rock seam thickness, dip angle, and other endowment conditions and coal seam mining layout. According to the way of dense grid arrangement in the key research area, the model adopts unequal division of cells and encrypts the grid distribution in the area of 600~800 m (100 m before and after the direction of the W1145 open cut lane) to the east of the central open cut lane along the direction of W1123 working face to reasonably simplify the model and improve the analysis speed of the program.

**3.2.2. Numerical Calculation Model Design.** The total design dimensions of the constructed model are 525 m in width in the  $x$ -direction, 400 m in height in the  $z$ -direction, and 1468 m in length in the  $y$ -direction. In the model, the displacements on the sides and bottom are restricted. To simulate the self-weight of the rock layer of loess, mudstone, sandstone, and sand conglomerate between the top of the model and the ground, a load of 5.4 MPa is applied to the upper surface rock layer to simulate the vertical stress acting on it by the overlying coal rock body, to make the established model more consistent with the actual situation.

The W1123 working face inclined length is 192 m, recoverable strike length is 1468 m, mining height is 3.2 m, coal release thickness is 6.3 m, average thickness is 9.5 m, working face inclination average of  $14^\circ$ , excavating the whole coal seam thickness, simulating comprehensive mining. The W1123 working face is located from 54 m to 236 m in the  $x$ -direction and 88 m to 136 m in the  $z$ -direction, and the working face advances along the  $y$ -direction.

For the accuracy of the simulation, the sequence of the model working face excavation is consistent with the actual back mining situation. The following are the main steps of the model excavation: overall excavation of the W1143 working face, excavation of the W1145 working face, excavation of the W1121 working face, and excavation of the W1123 working face transport lane and return air lane and then the back mining of the working face.

**3.3. Active Predictive Technology Implementation.** This kind of point prediction analysis lacks accuracy in evaluating the impact hazard of the whole working face, and it is difficult to meet the actual needs of the project. By dividing the working face into small cells, the prediction analysis is performed for each small cell separately to evaluate the impact hazard of the whole working face. Using the trained neural network model, the above-mentioned influencing factors are obtained based on the contours of the coal seam floor and geological reports of the study working face to predict the impact ground pressure hazard of the destination coal seam, and the impact ground pressure hazard level distribution of the study area is shown in Figure 4.

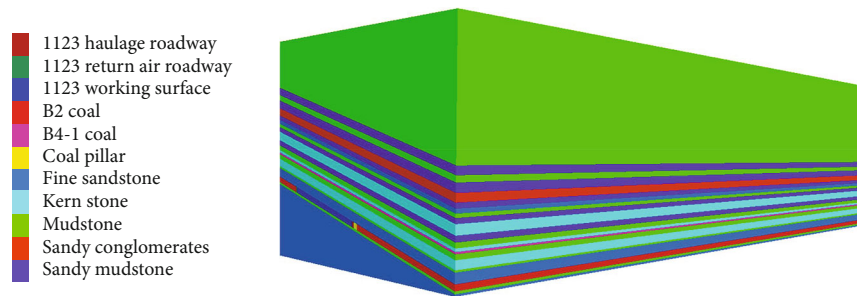


FIGURE 3: Numerical simulation model.

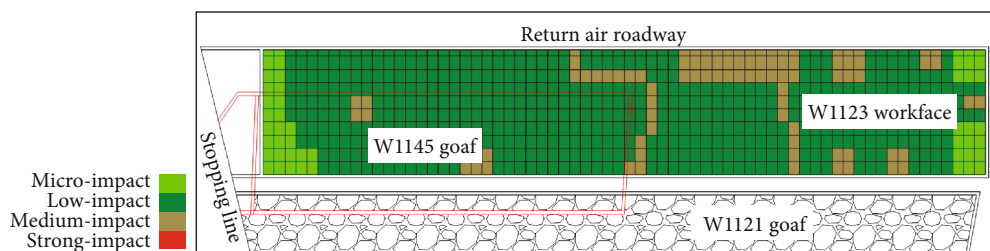


FIGURE 4: Distribution of impact hazard areas on the working face using the BP neural network model.

According to the established neural network prediction model, the impact ground pressure prediction results of the working face are mainly weak impact and medium impact hazards. When it is below the solid coal of W1145, the medium impact hazard in the area of 245~480 m in the middle and lower part of the working face is close to the transportation road, and the medium impact hazard in the area of 340~680 m in the middle and upper part of the working face is close to the return air road of the working face; when it is below the mining area of W1145, the predicted medium impact hazard area of the working face is concentrated between 700 and 980 m.

#### 4. Inversion Analysis of the “Time-Space-Strength” Characteristics of the Impact Ground Pressure Microseismic Monitoring Parameters

With the disturbance of coal and rock seams by workforce retrieval, the original rock stress balance is disrupted and stress redistribution is easy to form high-stress areas, which are high-frequency areas for inducing impact ground pressure. Mine in the W1143 working face back mining process in the back mining face had an impact ground pressure accident; this impact accident caused casualties and damage to the hydraulic support. The destruction process is accompanied by the generation, development, and penetration of fissures and then the breaking of coal and rock bodies and the destabilization of the structure, all with the release of energy. The analysis of monitoring data to explore the law of precursors when the impact ground pressure is revealed at the working face provides a reference basis for early warning and prevention of impact ground pressure at the working face.

##### 4.1. Characterization of Time Series Precursors of Microseismic Events for Impact Ground Pressure

4.1.1. “March 7, 2018,” Impact Event. On March 7, 2018, the cumulative advance distance of the transport lane of the W1123 working face was 68.0 m, and the cumulative advance distance of the return air lane was 80.0 m. The coordinates of the shock location of the large energy event at the working face were (354, 8826, 1331), and the highest single energy of  $3.10 \times 10^5$  J was monitored by microseismic. The overadvance precracking holes of the return air lane, intermediate process lane, and transport lane were blasted to 9.2 m, 50.0 m, and 71.0 m of the overrunning working face.

The spatial distribution of microseismic events of different energies on March 7 is shown in Figure 5. From the figure, it can be seen that the impact event occurred at the junction between the top of the coal seam and the rock seam on the side of the coal pillar of the haulage lane, 60.0 m ahead of the working face. In the area of 39.0 m in front of the working face in Figure 5(a), the distribution of microseismic events is less in this interval, and the main location of microseismic events is in the middle and lower part of the working face, and the concentration of microseismic energy events occurs at the place where the impact ground pressure occurs, and the density of energy events is significantly increased. According to the microseismic monitoring results in Figure 5(b), it can be seen that the rock damage developed from the low level to the high level, and the level of the surrounding rock activity has developed to the B3 coal seam. The impact event on March 7 was accompanied by a large sound, and after the large energy event, the inspection of the transport lane and the lower end head area of the working face caused a net pocket in the lower gang and shoulder nest of the 50~55 m section of the overrunning working face of the transport lane, and the impact large

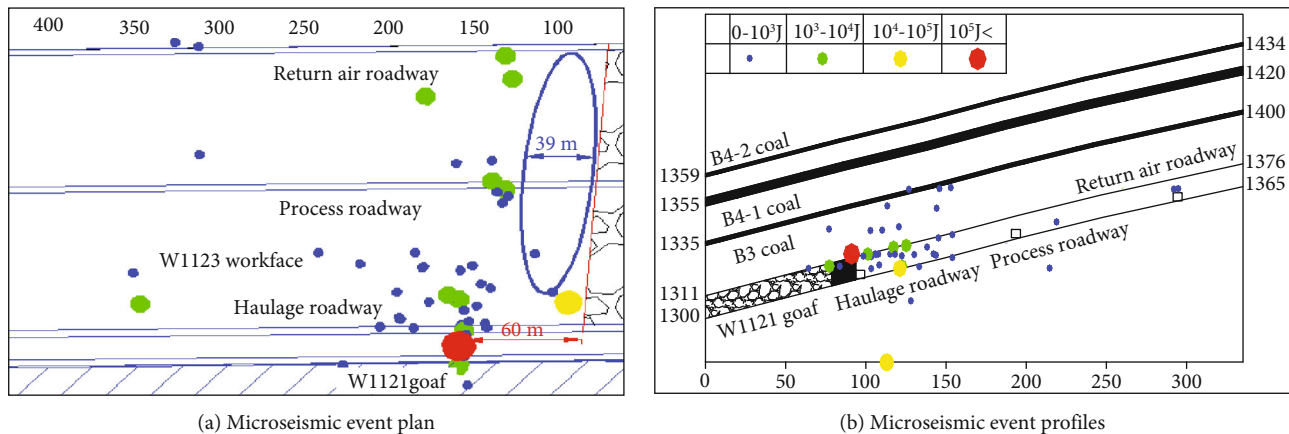


FIGURE 5: Spatial distribution of “March 7” microseismic events.

energy event occurred after the secondary small energy events occur frequently.

It shows the microseismic daily total energy-frequency distribution pattern. The number of microseismic events continued to decrease from February 28 to March 4, and the minimum value appeared on March 4, while the total daily energy of microseismic monitoring fluctuated narrowly around the low value of  $5.0 \times 10^4$  J between February 28 and March 5. When disturbed by external conditions, the sudden release of a large amount of accumulated energy can easily induce an impact on ground pressure disasters. The total energy and the number of events increased simultaneously after the 6th day, and the shock occurred on the 7th day, with a single release of microseismic energy reaching  $3.1 \times 10^5$  J. The total energy and the number of events increased as a whole, and the shock occurred again on the 8th day, with a single release of energy of  $6.2 \times 10^5$  J. The energy and the number of events changed dramatically on the 9th day, both of which were at low values, indicating that the energy in the coal rock body was effectively released after the two shocks. The number of events and the total energy of the microseismic daily monitoring showed a fluctuation of “down-up,” and the trend of change was in good agreement, so this impact event can be considered as a “V-shaped” impact event.

**4.1.2. “March 26, 2018,” Impact Event.** On March 26, 2018, the transport lane of the W1123 working face was advanced by 101.2 m in total and the return air lane was advanced by 106.4 m in total. A large energy event occurred at the working face with the coordinates of the shock source location (396, 8782, 1336) and single maximum energy of  $5.20 \times 10^5$  J. The return air lane, intermediate process lane, and transport lane overrun precracking holes were blasted to the overrun working face of 72.8 m, 60 m, and 86.8 m.

The spatial distribution of microseismic different energy events on March 26 is shown in Figure 6. The impact event occurred at the junction of the top of the coal seam and the rock seam, 18.3 m away from the lateral inclination of the coal wall of the haul roadway and 102.0 m ahead of the working face. As can be seen from Figure 6(a), the density

of microseismic events distributed in the middle and lower part of the working face (between the transport lane and the process lane) is greater than that in the middle and upper part of the working face (between the process lane and the return air lane); the distribution of microseismic events is less in the area of 43.0 m in the overrunning working face, mainly because the working face takes impact ground pressure prevention and control measures and overruns precracking blasting on the coal rock body in front of the working face in advance, and the microseismic events are far away from the working face. It indicates that the impact of ground pressure prevention and control has achieved a certain effect.  $10^3 \sim 10^5$  J events are mainly distributed on both sides of the roadway, mainly because the coal and rock bodies on both sides of the roadway are also subject to lateral support pressure; therefore, the impact ground pressure is easily induced on both sides of the roadway. From Figure 6(b), it can be seen that energy events at all levels are mainly distributed in the coal seam, and the seam of surrounding rock activity has developed to the  $B_{4-1}$  coal seam. The impact event was accompanied by a loud sound and strong vibration in the transportation lane, and secondary small energy events were frequent after the impact occurred. The impact caused the failure of 2 anchor rods in the transport lane, the roof of the lane was netted and the coal wall was flaky.

The trends of the total daily energy and number of microseismic events in the week before the shock event remain the same, with an undulating trend of increasing-decreasing-increasing. The trend of increasing microseismic energy and the number of events maintained from March 19 to March 22, with a significant increase in the number of events on the 24th, while the total energy remained at low values, indicating that the energy of a single event is decreasing and that there is a large amount of fracture development and development within the coal rock body. The impact ground pressure occurred on the 26th, and the energy and number of events decreased in the following days, indicating that the elastic energy accumulated in the coal rock body was released. The microseismic monitoring data of this impact event showed an overall “N”-type trend.

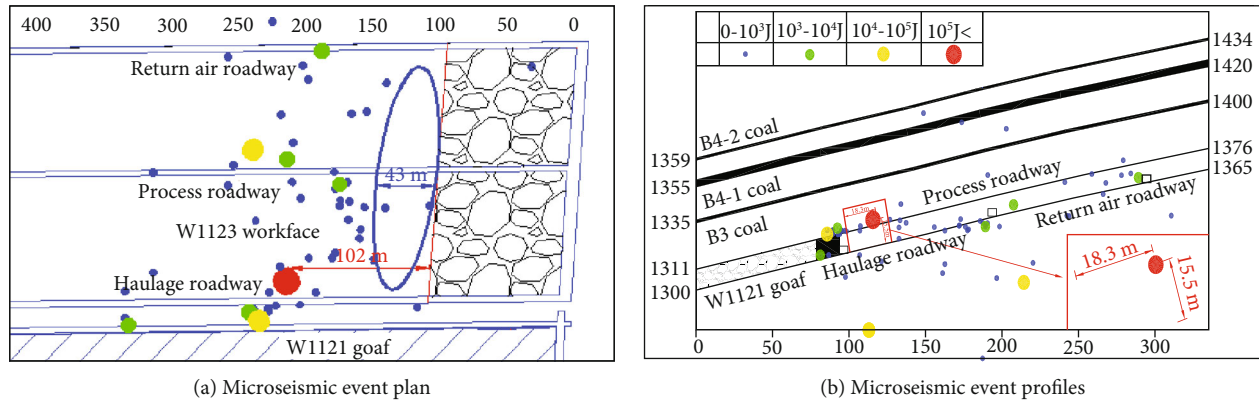


FIGURE 6: Spatial distribution of the “March 26” microseismic events.

**4.2. Analysis of the Precursor Characteristics of the Spatial Distribution of Microseismic Events of Impact Ground Pressure.** The vibration in the process of coal rock energy release is caused by mining disturbance and stress change in the coal mining process; these vibration events are likewise correlated in spatial distribution. Through the collation of microseismic monitoring data, the microseismic data are statistically analyzed in planar space to explore the precursor characteristics of their distribution in space. Due to the huge destructive nature of impact ground pressure, timely early warning can provide a reliable basis for the prevention and control of impact ground pressure. The microseismic monitoring data of the first 4 days of the impact large energy event occurred on the working face were selected, and the spatial distribution of the event was drawn to explore the characteristics of the microseismic events in the spatial distribution of the working face before the impact event occurred and to provide a reference basis for the prevention and control and early warning of the impact ground pressure on the working face.

Figure 7 shows the planar distribution pattern of large events of impact energy occurring on the working face. From the figure, it can be seen that the distribution of microseismic events on the working face has zoning characteristics, and the energy events are mainly concentrated in the middle and lower part of the working face, while the distribution of events in the middle and upper part is less and the event density is low. And the location of the impact of large energy events occurring in the working face is relatively concentrated, mainly occurring in the coal pillar of the transport lane of the working face and the lower working face 20~50 m away from the coal wall side of the transport lane. From Figures 7(a) and 7(b), it can be seen that the microseismic distribution in the middle and lower part of the working face during the 4 days before the occurrence of the impact large energy appears to the obvious low-density area of energy events, and the microseismic events of each energy level in this area decrease and the event density decreases.

The monitored microseismic events are mainly concentrated in the middle and lower part of the working face, and the energy events in the middle and upper part of the

working face are fewer and less dense, so it has a better prediction effect to use the phenomenon of the low density of energy events to predict the impact ground pressure in the middle and lower part of the working face, while the energy events monitored in the middle and upper part of the working face are few, and there are more blank areas of energy events in the spatial distribution. According to the field production practice, the middle and upper part of the working face after the impact pressure prevention and treatment was measured, the degree of danger is low and can be safely retrieved, and no impact large energy events have occurred, so the impact ground pressure warning precursor law of this method is more applicable to the middle and lower part of the working face. As the working face is retrieved, it is adjusted according to the monitoring results when it is located below the mining area.

## 5. Passive Warning Technique Based on the Combination of Dynamic Changes and Microseismic $b$ -Values

**5.1. Dynamic Rate of Change of Microseismic Indicators.** The destruction process of the coal rock body is the evolution process of stress redistribution, when the whole coal rock body is disturbed by mining, the structure of the coal rock body is destroyed, and the stress equilibrium state is broken to cause the structural instability of coal rock body, through the development of fracture, development, and structural breakage to release the elastic energy accumulated in the coal rock body. After the energy accumulated in the coal rock body is effectively released, the surrounding rock structure is in a new equilibrium stage, and the whole process is the cycle process of structural equilibrium-destabilization-equilibrium [21].

Through the collection of microseismic data from the working face by the microseismic online monitoring system, the change of stress in the coal and rock body is reflected by analyzing the change of relevant indexes of microseismic data, to understand the rupture, breakage, and destabilization of the coal and rock body of the working face in the process of recovery in time and to make fast and accurate



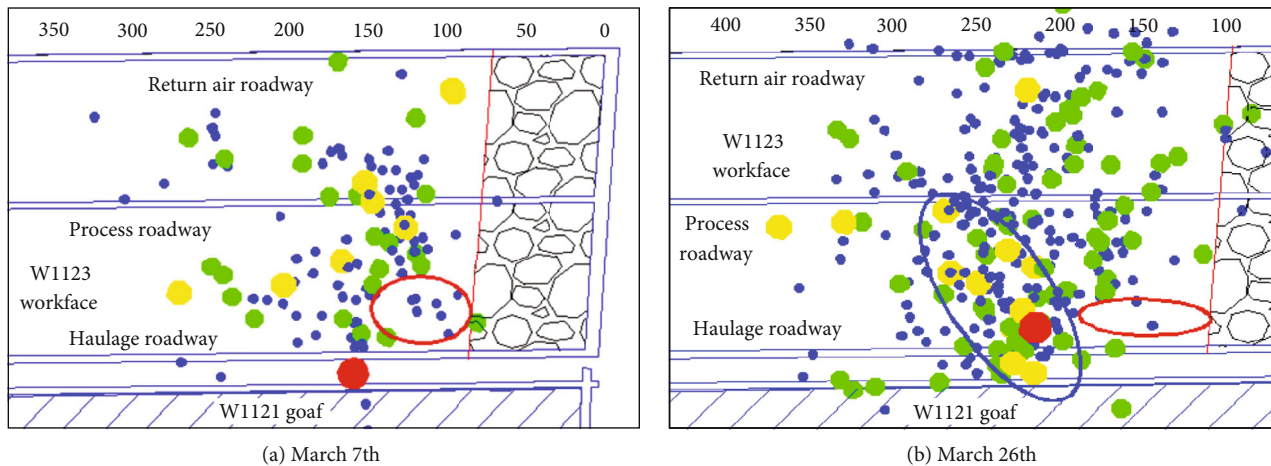


FIGURE 7: Spatial distribution characteristics of microseismic events before the occurrence of impact ground pressure.

decisions for abnormal conditions. The calculation formula of the change rate is as follows.

$$Q = \frac{M - N}{M} \times 100\%, \quad (1)$$

where  $M$  and  $N$  values are the values at the inflection point of microseismic signal fluctuation before the occurrence of shock, i.e., the maximum and minimum values in the rising or falling trend of the microseismic monitoring data signal.

By introducing the critical values of daily total energy, frequency and dynamic change rate sensitive indicators, the parameters of comprehensive early warning system of rock burst in Kuangou Coal Mine are determined. The early warning criteria of critical value method are as follows.

$P \leq P_{\min}$  or  $P \geq P_{\max}$ , exceeding the upper critical value, indicates that the activity of the coal rock body surrounding rock intensifies and a large amount of energy is released less than the lower critical value, the coal rock body is in the stage of energy accumulation, and the sudden release of accumulated energy is likely to induce disasters. When  $P$  is in the range between the lower critical value and the upper critical value is the safety interval, the range beyond the two is in the warning state.

**5.2. Microseismic Event  $b$ -Value Determination.** In this paper, the  $b$ -value in the “G-R” relationship is used as the characteristic index of microseismic [22]. By collecting the online monitoring data of microseismic, the time series scan analysis of the microseismic monitoring data of the Kuan Gou coal mine is carried out, and the linear least square method is usually used when the  $b$ -value is analyzed by time series scan.

Considering that the number of microseismic monitoring data smaller than the initial magnitude may be poorly recorded and incomplete due to various reasons, the starting magnitude needs to be given, while the number of high-magnitude microseismic events also has a large effect on the  $b$ -value. Therefore, data within a certain magnitude range are usually selected for the analysis of  $b$ -values. In

addition, errors in magnitude determination make it necessary to perform magnitude binning to ensure that the data within a certain magnitude bracket do not deviate too far from the actual distribution [23].

When evaluating the  $b$ -value, the microseismic data should be selected as the lower energy limit  $\Delta E$ , and the microseismic events within the appropriate magnitude range should be selected to evaluate the  $b$ -value. The geological conditions and retrieval process of each mine have variability, and the microseismic monitoring data of different mines and even different retrieval workings of the same mine have variability, and for the problem of selecting the energy range, based on the collated microseismic online monitoring data, the statistical microseismic data were evaluated. Based on the microseismic online monitoring data compiled, the statistical microseismic data were divided into energy classes with  $\lg E = 0.2$ , and the differences between the distribution characteristics of the monitoring data and the linear relationship of G-R were statistically analyzed to arrive at a reasonable range of microseismic energy values.

**5.3. Passive Warning Technology Implementation.** This paper focuses on the risk of impact ground pressure at the working face, analyzes the geological endowment perspective and mining disturbance perspective, and explores the degree of impact hazard and hazard range at the working face. At the same time, it analyzes the microseismic monitoring data to understand the spatial and temporal precursor characteristics of the microseismic monitoring data before the occurrence of impact ground pressure and lays the foundation for the establishment of the impact ground pressure warning method. Based on the prediction results of the neural network, the distribution of impact hazard area calculated by numerical simulation, and the precursor characteristics of microseismic online monitoring data, the critical value and dynamic rate of change were introduced to determine the critical value of impact ground pressure warning sensitive indicators and the trend method warning criterion for the Kuan Gou coal mine, and the impact ground pressure comprehensive warning method was constructed by

TABLE 6: Multi-indicator early warning method for impact ground pressure.

Methods	Hazard critical value or danger area range
BP neural network	The hazardous distribution area of impact ground pressure
Numerical simulation	Whether it is in the high-stress area
Spatial distribution characteristics of microseismic data	Whether there are obvious low-density areas
Total daily energy	$Q$ (dynamic rate of change) $\geq 60.0\%$ ; $P_{\max} \geq 1.5 \times 10^5$ J; $P_{\min} \leq 5.0 \times 10^4$ J
Daily frequency	$Q$ (dynamic rate of change) $\geq 30.0\%$ ; $P_{\max} \geq 60$ ; $P_{\min} \leq 30$
$b$ -value	$b \leq 0.457$
Judging method	<p>(1) When the working face is in the danger area predicted by BP neural network or numerical simulation, it means that the predicted indicators of these two methods issue early warning, where the weak impact danger predicted by the BP neural network is indicated by 1 unit of early warning indicator, and the medium impact danger is indicated by 2 units of early warning indicator. For other indicators beyond the critical value range or in the danger region, it is recognized that the indicator issued a warning; the warning level will be divided into four levels: A level: 1~2 indicators warning; B level: 3~4 indicators warning; C level: 5~6 indicators warning; and D level: greater than 7 indicator warning</p> <p>(2) According to the comprehensive results of BP neural network and numerical simulation, analyze whether the location of the working face is in the circled I, II, III, IV, V of these five high-risk areas; when back mining these areas, the actual production should strengthen the monitoring, prevention, and control</p>

selecting the warning indicators to realize the “critical + trend” multiparameter warning method for impact ground pressure hazard. By selecting the early warning indicators and constructing the comprehensive early warning method, we can realize the comprehensive early warning with multiple parameters and indicators for the “criticality” and “trend” of the impact pressure hazard, so that the comprehensive early warning method can be more accurate and provide a reliable basis for the prevention and control of the impact hazard at the working face.

## 6. Construction and Application of Impact Ground Pressure Resilience Prevention System

**6.1. Ductile Impact Ground Pressure Prevention System.** Impact pressure is one of the main disasters affecting coal mine safety production, and the early warning of impact pressure is the basis for taking prevention and control measures, which is of great research significance to ensure the safety of underground personnel, the integrity of equipment, and the normal recovery of the working face. The reliability of single-indicator prediction analysis is not guaranteed, and the effect error is large. Multi-indicator integrated early warning can more comprehensively assess the degree of impact hazard at the working face, improve the accuracy of early warning, and serve as the basis for the construction measures to prevent and relieve pressure. The multiparameter integrated warning is an important research direction for impact ground pressure prevention and control.

According to the actual production situation of the Kuan Gou coal mine, the BP neural network was selected to predict the impact hazard of the working face by region; the evolution law of the retrieval stress of the working face

was summarized and analyzed by numerical simulation, and the high-stress concentration distribution area was circled; the monitoring data of the microseismic online monitoring system was selected to make statistical analysis of the corresponding indexes. According to the comprehensive early warning principle of “critical + trend” of impact pressure hazard, the comprehensive early warning method of impact pressure applicable to the Kuan Gou coal mine was determined. Comprehensive early warning methods are shown in Table 6.

## 6.2. Effectiveness Testing and Evaluation

**6.2.1. Description of Impact Ground Pressure Event.** On September 10, 2018, the transport lane of the W1123 working face was advanced by 368.4 m in total, and the return air lane was advanced by 372.0 m in total. This time, a large-energy event occurred at the working face with the coordinates of the shock source location (609, 8687, 1346) and the highest single energy of  $9.5 \times 10^5$  J. The return air lane, intermediate process lane, and transport lane overrun pre-cracking holes were blasted to the overrunning working face 129.8 m, 127 m, and 153.2 m.

The spatial distribution of microseismic different energy events on September 10 is shown in Figure 8, from which it can be seen that the impact events occurred in the rock seam 60.0 m ahead of the working face, 20.0 m upward from the coal wall side of the roadway, and 10.0 m vertically upward from the top of the coal seam. In Figure 8(a), the microseismic events are mainly concentrated in the middle and lower part of the working face, and there is a concentration of microseismic energy events at the place where the impact ground pressure occurs, and the density of microseismic energy events is higher than other areas of the working face, and the structure of the coal rock body in front has been

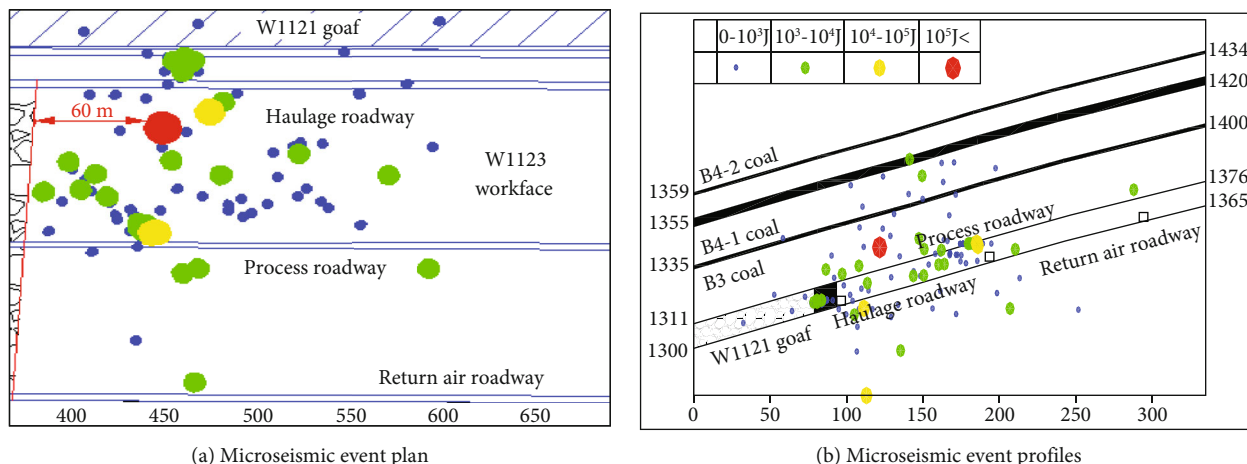


FIGURE 8: Spatial distribution of the “September 10” microseismic events.

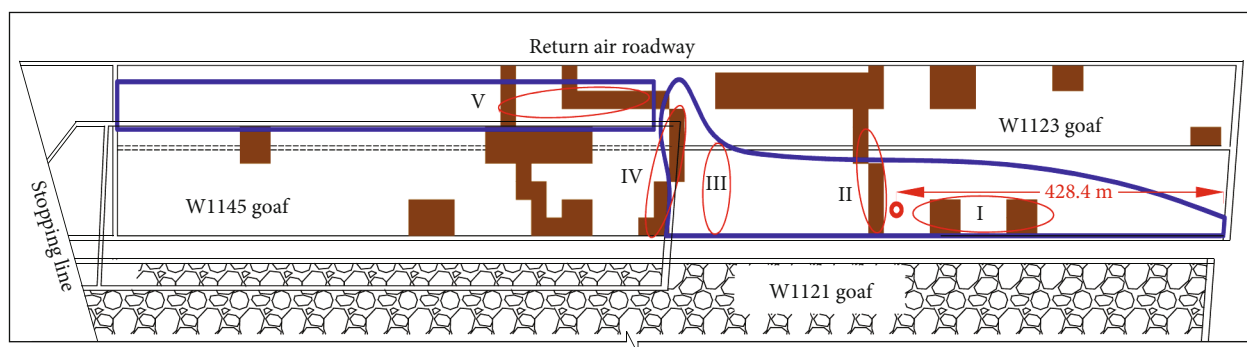


FIGURE 9: Distribution of impact ground pressure hazard areas.

damaged; according to the microseismic monitoring results in Figure 8(b), the energy events are mainly concentrated between the return air lane and the process lane. According to the microseismic monitoring results in Figure 8(b), the energy events of  $10^3 \sim 10^5$  J were mainly concentrated in the coal seam and the rock seam within 10.0 m from the coal seam intersection, and the damage of the rock seam was developed from the low level to the high level, and the level of the surrounding rock activity had developed to the  $B_{4-1}$  coal seam, with a large development height and a wide impact range, and the distribution in space was “parabolic.” The impact situation is as follows: large energy events occur with a loud sound, and strong vibration in the transportation lane and secondary small energy events occurs frequently after the occurrence of large energy events. There were 2 broken anchors and 5 failed anchors at the impacted lane, and the roof of the transport lane sank 30~40 cm near the impacted location, and two net pockets appeared, sinking about 80 cm.

6.2.2. Response of Each Monitoring Indicator

(1) *The BP Neural Network and Numerical Simulation of the Response of Hazardous Area Indicators.* The W1123 working

face transport lane has advanced 368.4 m and the return air lane has advanced 372.0 m, the working face is located in the I area of the 5 high-risk areas circled, which is a high-risk area of impact as determined by geological conditions and mining disturbance conditions, and the impact event is 60.0 m ahead of the working face, which is close to the designated risk II area, as shown in Figure 9. The details are shown in Figure 9. Although the impact location is close to the II high-risk area, not completely located in the II area, the impact prediction effect of the “trend method” warning index response effect is better and can provide a reference for impact warning.

(2) *Response of Spatial Distribution Indicators of Microseismic Energy Events.* The spatial distribution characteristics of microseismic energy events are shown in Figure 10. There are two low-density areas of microseismic events in the middle and lower part of the working face within 4 days before the occurrence of large impact energy, one is in the area between the impact event location and the coal wall of the mining face, and the other is in the area 40~115 m eastward along the strike of the impact event location. In these two areas, there are fewer microseismic events of each energy level, and the event density decreases, and then, the shock

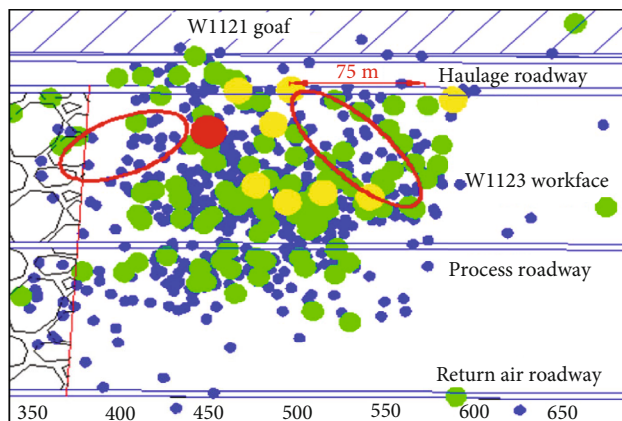


FIGURE 10: Spatial distribution of microseismic data before the occurrence of impact ground pressure.

event occurs in the middle of the two event low-density areas, while the microseismic events with the energy of  $10^4\sim 10^5$  J represented in yellow are also concentrated between the two low-density areas, indicating that the microseismic event spatial low-density indicator has responded a few days before the occurrence of the shock ground pressure, and this phenomenon has good sensitivity as an early warning indicator with good sensitivity.

(3) *Response of Daily Total Energy-Frequency Index.* There is a more obvious precursor reflection of daily total energy frequency before the impact event occurred on September 10, 2018, and the number of microseismic events from September 2 to September 5 showed a large fluctuating change, and the number of energy events on the 5th showed a peak reaching 235, during which the daily total energy was in a more stable state, with the total energy fluctuating at  $1.8 \times 10^5$  J. Based on the analysis relationship of daily total energy-frequency, the observation position data are from 5th to 9th, and the monitoring data of them are in good consistency, and the total energy and the number of events both appear to be minimal on the 7th, and then both appear to increase in the trend, and the impact event occurs on the 10th. Using the dynamic rate of change calculation method proposed earlier, the dynamic rate of change of total energy and frequency on the day before the shock event was 64.5% and 49.3%, respectively. Both dynamic rates of change indicators exceeded the threshold values of the warning indicators, indicating that both indicators had given warning signals before the occurrence of the shock event.

(4) *Response of  $b$ -Value Indicators.* According to the online monitoring data, the data were processed to obtain the changing trend of the  $b$ -value for a while before the impact event. The change of  $b$ -value fluctuated greatly for a while before the impact event on September 10, and the  $b$ -value was less than the warning threshold on September 1, 2, and 9, indicating that the  $b$ -value warning of selected microseismic data has a certain reference value for the prediction and warning of impact ground pressure.

Therefore, all the indicators have warning signals for the impact ground pressure accident that occurred on “September 10, 2018,” and there are 7 indicators that meet the warning conditions, and the impact event belongs to the D-level impact according to the established comprehensive multiparameter warning evaluation method. The early warning situation is in good agreement with the practice, indicating that the established early warning method can meet the practical needs and can provide a reference for the prevention and control of impact ground pressure.

## Data Availability

All data included in this study are available upon request by contact with the corresponding author.

## Conflicts of Interest

The authors have no conflicts of interest to declare.

## Acknowledgments

This work was supported by the National Natural Science Foundation of China (Grant No. 51874231).

## References

- [1] N. M. Michieka, “Energy and the environment: the relationship between coal production and the environment in China,” *Natural Resources Research*, vol. 23, no. 2, pp. 285–298, 2014.
- [2] J. P. Sun and X. H. Qian, “Analysis of coal mine accidents in China during 2004–2015,” *Industry and Mine Automation*, vol. 42, no. 11, pp. 1–5, 2016.
- [3] Y. Xue, P. G. Ranjith, F. Dang et al., “Analysis of deformation, permeability and energy evolution characteristics of coal mass around borehole after excavation,” *Natural Resources Research*, vol. 29, no. 5, pp. 3159–3177, 2020.
- [4] L. H. Tan, T. Ren, L. M. Dou, X. H. Yang, M. Qiao, and H. D. Peng, “Analytical stress solution and mechanical properties for rock mass containing a hole with complex shape,” *Theoretical and Applied Fracture Mechanics*, vol. 114, p. 103002, 2021.
- [5] L. Laurent, D. Christian, and R. Philiippe, “Comparison of the anisotropic behaviour of undeformed sandstones under dry and saturated conditions,” *Tectonophysics*, vol. 370, no. 1–4, pp. 193–212, 2003.
- [6] A. G. Grant, “Fluid effects on velocity and attenuation in sandstones,” *Journal of the Acoustical Society of America*, vol. 96, no. 2, pp. 1158–1173, 1994.
- [7] M. Rezaei, M. F. Hossaini, and A. Majdi, “A time-independent energy model to determine the height of distressed zone above the mined panel in longwall coal mining,” *Tunnelling and Underground Space Technology*, vol. 47, pp. 81–92, 2015.
- [8] L. Shi, Y. Wang, M. Qiu, L. Han, and Y. Zhao, “Research on the required width of a fault waterproof coal pillar based on underground pressure control theory,” *Arabian Journal of Geosciences*, vol. 12, no. 15, pp. 1–14, 2019.
- [9] A. H. Wilson, “The stability of underground workings in the soft rocks of the coal measures,” *International Journal of Mining Engineering*, vol. 1, no. 2, pp. 91–187, 1983.



- [10] L. H. Ma, X. Jiang, J. Chen, Y. F. Zhao, R. Liu, and S. Ren, "Analysis of damages in layered surrounding rocks induced by blasting during tunnel construction," *International Journal of Structural Stability and Dynamics*, vol. 21, no. 7, article 2150089, 2021.
- [11] P. Bukowski, "Water hazard assessment in active shafts in upper Silesian coal basin mines," *Mine Water and the Environment*, vol. 30, no. 4, pp. 302–311, 2011.
- [12] R. Wang, J. B. Bai, S. Yan, Z. G. Chang, and X. Y. Wang, "An innovative approach to theoretical analysis of partitioned width & stability of strip pillar in strip mining," *International Journal of Rock Mechanics and Mining Sciences*, vol. 129, article 104301, 2020.
- [13] W. Liang, G. Zhao, X. Wang, J. Zhao, and C. Ma, "Assessing the rockburst risk for deep shafts via distance-based multi-criteria decision making approaches with hesitant fuzzy information," *Engineering Geology*, vol. 260, article 105211, 2019.
- [14] S. Wang, X. Li, and D. Wang, "Mining-induced void distribution and application in the hydro-thermal investigation and control of an underground coal fire: a case study," *Process Safety and Environment Protection*, vol. 102, pp. 734–756, 2016.
- [15] P. Wen-qing, W. Wei-jun, and L. Qing-feng, "Reasonable width of waterproof coal pillar under the condition of different fault dip angles," *Journal of Mining & Safety Engineering*, vol. 26, no. 2, pp. 179–186, 2009.
- [16] Y. Chen, G. Zhao, S. Wang, H. Wu, and S. Wang, "A case study on the height of a water-flow fracture zone above undersea mining: Sanshandao Gold Mine, China," *Environmental Earth Sciences*, vol. 78, no. 4, p. 122, 2019.
- [17] Z. J. Wen, S. L. Jing, Y. J. Jiang et al., "Study of the Fracture Law of Overlying Strata under Water Based on the Flow- Stress-Damage Model," *Geofluids*, vol. 2019, Article ID 3161852, 12 pages, 2019.
- [18] W. A. N. G. Shao-feng, T. A. N. G. Yu, L. I. Xi-bing, and D. Kun, "Analyses and predictions of rock cuttabilities under different confining stresses and rock properties based on rock indentation tests by conical pick," *Transactions of Nonferrous Metals Society of China*, vol. 31, no. 6, pp. 1766–1783, 2021.
- [19] S.-f. Wang, Y. Tang, and S.-y. Wang, "Influence of brittleness and confining stress on rock cuttability based on rock indentation tests," *Journal of Central South University*, vol. 28, no. 9, pp. 2786–2800, 2021.
- [20] L. Bo and Y. J. G. Chen, "Risk assessment of coal floor water inrush from underlying aquifers based on GRA-AHP and its application," *Engineering Geology*, vol. 34, no. 1, pp. 143–154, 2016.
- [21] Y. L. Tan, F. H. Yu, and L. Chen, "A new approach for predicting bedding separation of roof strata in underground coal-mines," *International Journal of Rock Mechanics and Mining Sciences*, vol. 61, pp. 183–188, 2013.
- [22] X.-P. Lai, S. Zhang, P.-F. Shan, F. Cui, Y.-B. Yang, and R. Bai, "Experimental study of unconventional modified filling energy absorption and control mechanism in high energy storage rock masses," *Scientific Reports*, vol. 12, article 11783, 2022.
- [23] Feng, E. K. Hou, X. S. Xie, and P. F. Hou, "Research on Water-conducting Fractured Zone height under the condition of large mining height in Yushen mining area, China," *Lithosphere*, vol. 1, 2023.